Chemical Engineering Journal 146 (2009) 498–502

Contents lists available at ScienceDirect

Chemical Engineering Journal

journal homepage: www.elsevier.com/locate/cej

Synthesis and characterization of ZnO nanocrystals from thermolysis of new precursor

Masoud Salavati-Niasari[a,b,*], Fatemeh Davar[b], Zeinab Fereshteh[a]

[a] Institute of Nano Science and Nano Technology, University of Kashan, P. O. Box 87317-51167, Kashan, Islamic Republic of Iran
[b] Department of Chemistry, Faculty of Science, University of Kashan, P. O. Box 87317-51167, Kashan, Islamic Republic of Iran

ARTICLE INFO

Article history:
Received 1 July 2008
Received in revised form
16 September 2008
Accepted 23 September 2008

Keywords:
Nanostructures
Synthetic methods
Zinc oxide

ABSTRACT

ZnO nanocrystals were prepared by the thermolysis of Zn–surfactant complexes. The particle sizes of the nanocrystals were from 15 to 25 nm. The products were characterized by X-ray diffraction (XRD), scanning electron microscopy (SEM), transmission electron microscopy (TEM), high-resolution transmission electron microscopy (HRTEM), energy dispersive X-ray (EDX), X-ray photoelectron spectroscopy (XPS), Fourier transform infrared (FT-IR) spectroscopy and ultraviolet–visible (UV–vis) spectroscopy. The synthesized ZnO nanocrystals have a hexagonal wurtzite structure.

1. Introduction

In recent years, there has been an increasing interest in developing materials with low-dimensional nanostructure such as nanotubes and nanocrystals due to their potential technological application in nanoscale devices [1–4]. It has been obvious that their properties depend sensitively on their size and shape. Therefore, the challenges in the synthesis of nanocrystals are to control not only the crystal size but also the shape and morphology [5,6].

ZnO is a direct gap semiconductor with a large band gap of 3.37 eV and a large exciton binding energy of 60 meV. The strong exciton binding energy can ensure an efficient ultraviolet–blue emission at room temperature. Accordingly, ZnO nanocrystals have great potential in applications such as laser diodes [7], solar cells [8,9], sensors [10] and catalysts for liquid phase hydrogenation [11].

In the past decade, various different physical or chemical synthetic approaches have been developed to produced ZnO, including vapor phase oxidation [12], thermal vapor transport and condensation (TVTC) [13,14], polyol methods [15], precipitation [16–18], sol–gel [19,20], microemulsion [21], hydrothermal [22], solvothermal [23] and sonochemical methods [24].

Among various techniques for synthesis of ZnO nanoparticles, thermal decomposition is one of the most common methods to produce stable monodisperse suspensions with the ability of self-assembly. Nucleation occurs when the metal precursor is added into a heated solution in the presence of surfactant, while the growth state take place at a higher reaction temperature [25]. ZnO nanostructures can also be synthesized from different precursor [26,27]. Choi et al. [28] reported a method for the large-scale synthesis of uniform-sized hexagonal pyramid-shaped ZnO nanocrystals by the thermolysis of Zn–oleate complex. Zinc acetylaceton has been reported to be a good precursor for ZnO nanoparticles from thermal decomposition. More recently our group [29] has synthesized uniform ZnO nanoparticles with size 12 nm by thermal decomposition of zinc acetylacetonate in oleylamine. And so, monodisperse ZnO nanoparticles were successfully prepared through the decomposition of zinc acetylacetonate precursor by Jiang et al. [30]. With this thermolysis method, the utilization of simple, facile, cheap, air-stable, and less-toxic molecular precursors is expected to greatly facilitate the large-scale production of oxide nanocrystals for the above applications. A major interest at the moment is in the development of organometalic or inorganic compound for preparation of nanoparticles. Using of the novel compound can be useful and open a new way for preparing nanomaterials to control nanocrystal size, shape and distribution size.

Herein, we report on the facile synthesis of ZnO nanocrystals via thermolysis of new precursor ([bis(2-hydroxyacetophenato)zinc(II)]) in coordinating solvent oleylamine and triphenylphosphine (TPP). To the best of our knowledge, this is the first report on the synthesis of zinc oxide nanocrystals with this precursor. In this process, oleylamine was used as both the medium and the stabilizing reagent.

* Corresponding author. Tel.: +98 361 5555333; fax: +98 361 5552935.
E-mail address: salavati@kashanu.ac.ir (M. Salavati-Niasari).

1385-8947/$ – see front matter © 2008 Elsevier B.V. All rights reserved.
doi:10.1016/j.cej.2008.09.042

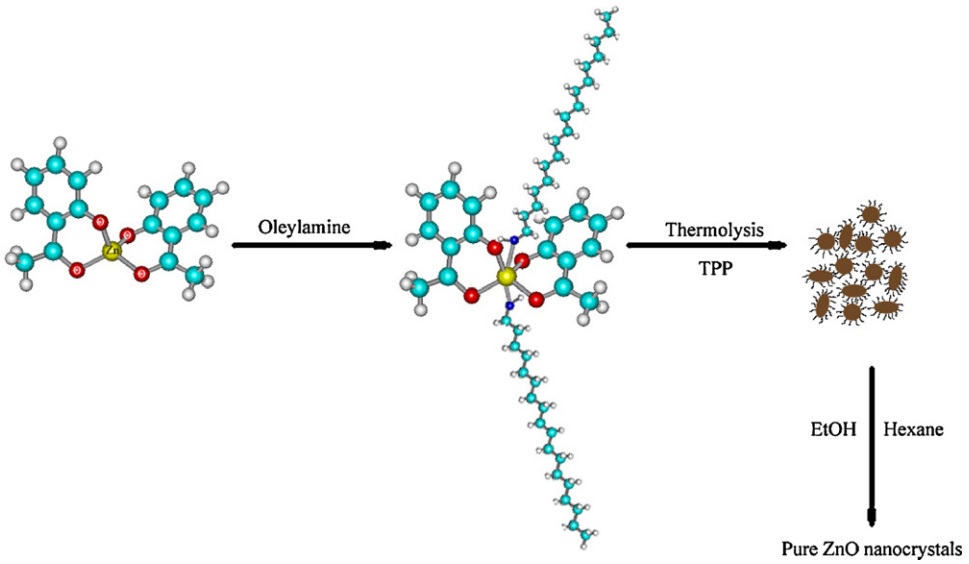

Scheme 1. Schematic depiction of the selective formation of ZnO nanocrystals. (For interpretation of the references to color in this artwork, the reader is referred to the web version of the article.)

2. Experimental

2.1. Materials

The precursor complex [bis(2-hydroxyacetophenato)zinc(II)], [Zn(aceto)$_2$], was prepared according to the procedure described previously [31]. Oleylamine, triphenylphosphine (TPP), toluene, hexane, and ethanol were purchased from Aldrich and used as received.

2.2. Characterization

XRD patterns were recorded by a Rigaku D-max C III, X-ray diffractometer using Ni-filtered Cu Kα radiation. Elemental analyses were obtained from Carlo ERBA Model EA 1108 analyzer. Scanning electron microscopy (SEM) images were obtained on Philips XL-30ESEM equipped with an energy dispersive X-ray spectroscopy. Transmission electron microscopy (TEM) images and electronic diffraction (ED) pattern were obtained on a Philips EM208 transmission electron microscope with an accelerating voltage of 200 kV. The high-resolution transmission electron microscopy (HRTEM) image and energy dispersive X-ray (EDX) were recorded on a JEOL-2010 TEM at an acceleration voltage of 200 kV. X-ray photoelectron spectroscopy (XPS) of the as-prepared products was measured on an ESCA-3000 electron spectrometer with nonmonochromatized Mg Kα X-ray as the excitation source. Fourier transform infrared (FT-IR) spectra were recorded on Shimadzu Varian 4300 spectrophotometer in KBr pellets. The electronic spectra of the complexes were taken on a Shimadzu UV–visible scanning spectrometer (Model 2101 PC).

2.3. Synthesis of ZnO nanocrystals

The current synthetic procedure is a modified version of the method developed by Hyeon group for the synthesis of various nanoparticles of metals and oxides, which employ the thermal decomposition of metal–surfactant complexes in hot surfactant solution [32]. The synthetic pathway is shown in Scheme 1. In the typical synthesis, a stock solution of Zn–surfactant complex, prepared by reacting 0.6 g of [Zn(aceto)$_2$] with 5 mL of oleylamine at 130 °C, was slowly injected into 5 g of triphenylphosphine (TPP) under vigorous stirring at 240 °C. The reaction temperature was then decreased to 230 °C and the resulting solution was stirred at this temperature for 1 h. The initial yellow color of the solution slowly turned brownish black, indicating that nanoparticles were generated. The reaction mixture was then cooled to

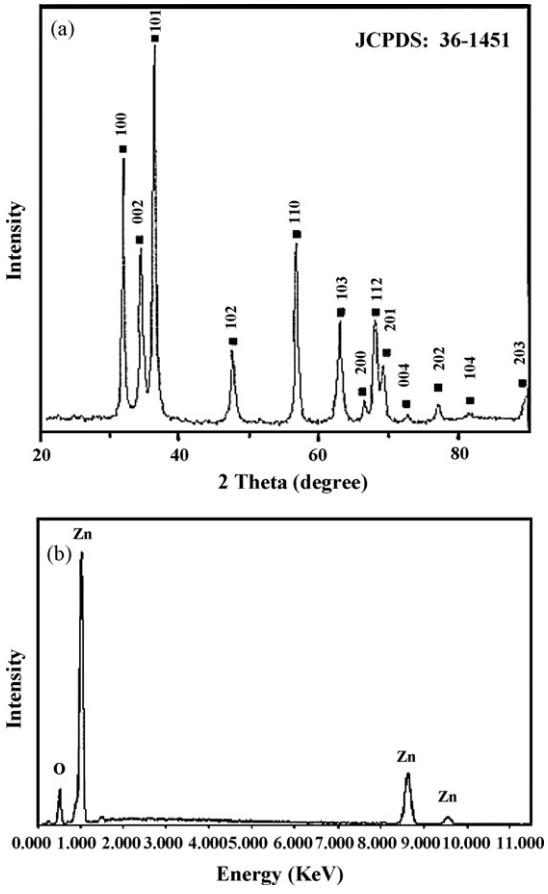

Fig. 1. (a) XRD pattern of the ZnO nanocrystals and (b) EDX spectrum of the ZnO nanocrystals.

room temperature, and the white nanoparticles were retrieved by adding 30 mL of anhydrous ethanol, followed by centrifugation. The final products were washed with ethanol for at least three times to remove impurities, if any, and dried at 100 °C. The retrieved powder of the nanoparticles could be easily redispersed in nonpolar organic solvents such as hexane or toluene (Scheme 1).

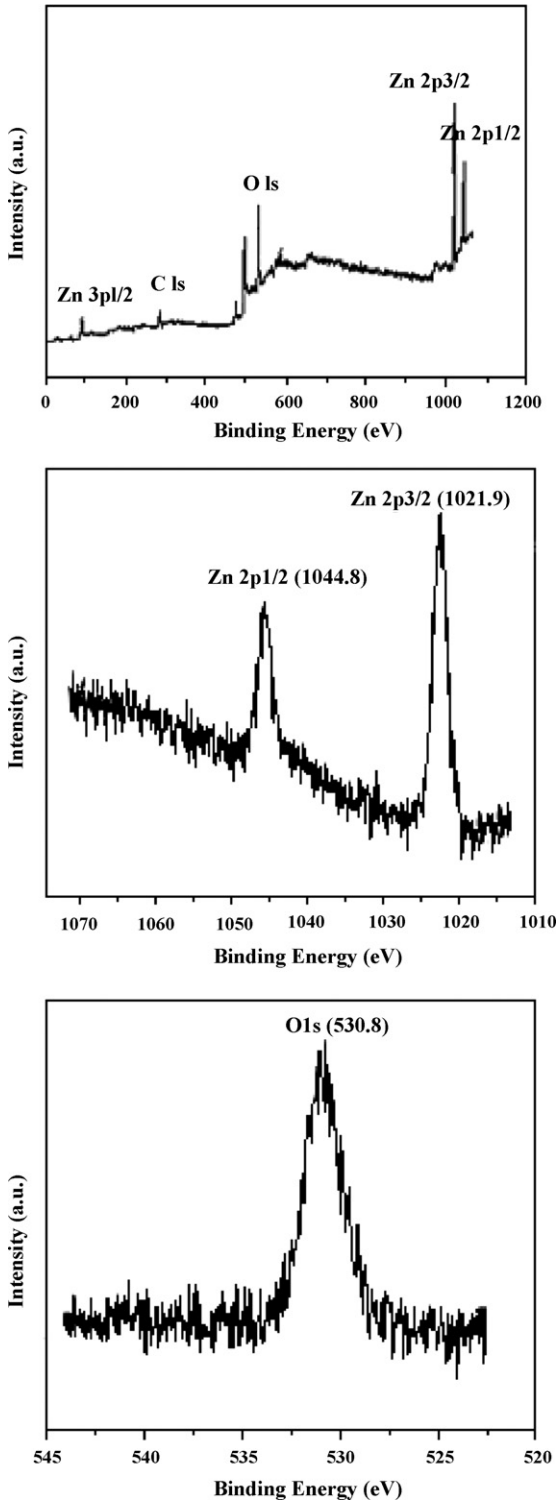

Fig. 2. X-ray photoelectron spectroscopy (XPS) of the as-synthesized ZnO nanocrystals.

3. Results and discussion

X-ray powder diffraction (XRD) pattern of the as-prepared sample is shown in Fig. 1a. The XRD pattern is consistent with the spectrum of ZnO, and no peak attributable to possible impurities is observed. The reflections of pure ZnO can be indexed well to hexagonal wurtzite ZnO (space group: $P6_3mc$; JCPDS No. 36-1451). The sharp diffraction peaks manifest that the obtained ZnO nanocrystals have high crystallinity. The size of the crystallite was estimated from Debye–Scherrer equation is about 12 nm. Chemical purity and stoichiometry of the samples were tested by EDX. The EDX image of nanocrystals (Fig. 1b) showed that components of the crystals are Zn and O with a ratio of 1:1.05.

Further evidence for the purity and composition of the products was obtained by X-ray photoelectron spectra (XPS). Fig. 2 shows the XPS of the as-prepared sample. The binding energies obtained in the XPS analysis were corrected for specimen charging by referencing the C 1s to 284.60 eV. The binding energies of O 1s, Zn $2p_{1/2}$, and Zn $2p_{3/2}$ provided a fairly complete picture of the sample powder. The Zn $2p_{3/2}$ XPS peak that appears at 1021.9 eV coincides with the findings for ZnO. The O 1s peak at 530.8 eV is attributed to the (O^{-2}) in the ZnO.

In order to further confirm that we have obtained fine-quality ZnO nanocrystals, supplementary experiments have been carried out on FT-IR spectra. Fig. 3 shows FT-IR spectrum for ZnO nanocrystals. The strong peak around 434 cm^{-1} shows a distinct stretching mode of crystal ZnO. The weak peaks at 3432 cm^{-1} has been assigned to the ethanol used in the separation step. The spectra of ZnO nanocrystals, shows two very weak stretch vibrations at 2924 and 2865 cm^{-1} attributing to the C–H stretching models of the oleylamine carbon chain, indicating oleylamine molecules are absorbed on the surface of ZnO nanocrystals. If there is adsorption of [Zn(aceto)$_2$] on the surface of the ZnO particles, a distinct carbonyl peak around 1640 cm^{-1} should appear in the FT-IR spectrum. So the oleylamine serves as the capping ligand that controls growth [33].

The morphology of the product is examined by SEM. Typical SEM image of as-obtained wurtzite ZnO nanocrystals is shown in Fig. 4 as well as the TEM images and ED pattern for detail illustration. Fig. 4a shows the SEM image of the as-obtained nanocrystals with spherical shape. The TEM images of the nanocrystals are shown in Fig. 4b. It reveals the nanocrystals with diameters ranging from 15 to 25 nm. The diameters of the products are in good agreement with those calculated by XRD patterns. The ED pattern (Fig. 4c) indicates that the ZnO nanocrystals are single-crystalline. This high-resolution TEM (HRTEM) image of a nanoparticle revealed the highly crys-

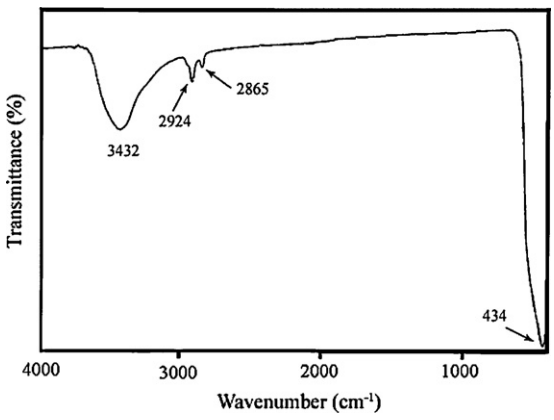

Fig. 3. FT-IR spectra of ZnO nanocrystals.

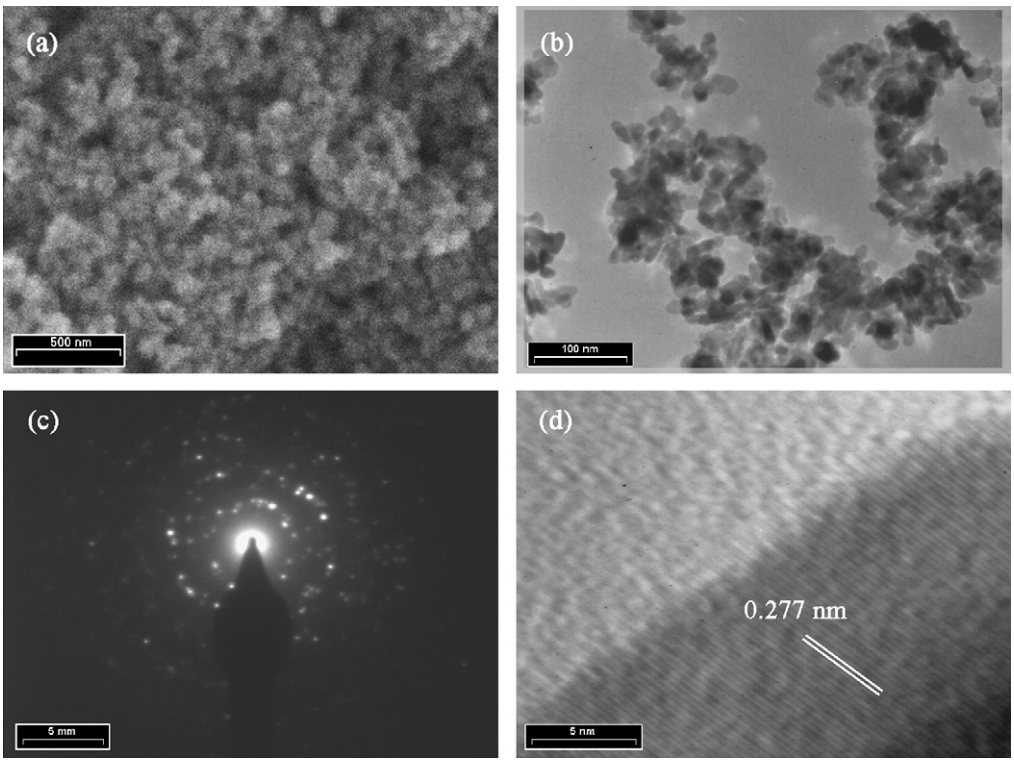

Fig. 4. Morphologies of the products: (a) SEM image; (b) TEM image; (c) ED pattern; (d) HRTEM image of the ZnO nanocrystals.

talline nature of the nanoparticles. The HRTEM image of a single ZnO nanoparticle showed that the nanoparticles were highly crystalline. In the HRTEM image (Fig. 4d), the distance between the two adjacent planes, *d*, is measured to be 0.277 nm.

The growth mechanism could be well understood on the basis of the following reactions and the crystal habits of hexagonal ZnO. In the presence of oleylamine as solvent [$Zn(aceto)_2$]-oleylamine were synthesized. After addition of TPP to these solutions at high temperature [$Zn(aceto)_2$]-oleylamine will decomposed. TPP was widely used in the synthesis of phosphine-stabilized gold or other metal nanoparticles. The phenyl groups in TPP can provide greater steric hindrance than straight-chained alkyl groups such as tributyl and trioctyl to control the size of metal nanoparticles [34]. The addition of TPP into the mixture of oleylamine and complex as an additional surfactant reduced the particle size much further and resulted in nanocrystals with very thin arrays. Oleylamine is known as a ligand that binds tightly to the metal nanoparticles surface. The combined effects of TPP and oleylamine were much more profound than those of individual contributions. On the other hand these complexes transform to ZnO [35]. When the triphenylphopsphine (TPP) was used as the complexing agent, the circumference of metallic nuclei was capped by this surfactant, leading to the increase of surface energy of some crystallographic faces. The growth of the ZnO nanocrystals can be explained on the basis of the schematic view presented in Scheme 1. The ZnO nanocrystals agglomerated together to form a hexagonal nucleus [36].

Optical properties of the ZnO nanocrystals were investigated by UV–vis spectroscopy and photoluminescence (PL) spectroscopy at room temperature (Fig. 5). Fig. 5a curve illustrates the UV–vis absorption spectrum of the nanocrystals, with exciton absorption peak at 365.5 nm, which has a large blue shift compared to that of bulk ZnO. Fig. 5b illustrates room-temperature photoluminescence (PL) spectra of ZnO. The PL spectra were recorded with an excitation of the 325 nm. According to literature [37], ZnO usually exhibits two strong emission peaks, near-band-edge and green broad-band, respectively. The near-band-edge emission peak is attributed to the direct recombination of excitons through an exciton–exciton collision process while the green broad-band emission peak origi-

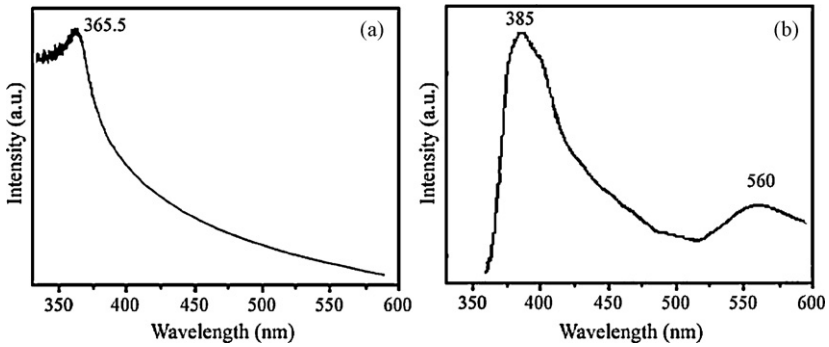

Fig. 5. (a) UV–vis absorption and (b) room temperature PL spectra of the ZnO nanocrystals.

nated from singly ionized oxygen vacancies and other point defects. Strong emission at 385 nm was detected in Fig. 5b, which comes from recombination of excitonic centers in the nanoparticles. The green emission (~558 nm) of ZnO comes from the recombination of electrons in singly occupied oxygen vacancies with photoexcited holes.

4. Conclusion

In conclusion, we synthesized crystalline ZnO nanocrystals in large quantity by the thermolysis of zinc acetophenato in oleylamine and triphenylphosphine under mild conditions. The crystallite size of the nanocrystals can be estimated between 15 and 25 nm. Since the precursor used is cheap, air-stable, and readily available for many metal elements, this synthesis may represent a rather environmentally friendly and general approach towards many other metal-oxide nanocrystals.

Acknowledgement

Authors are grateful to council of University of Kashan for providing financial support to undertake this work.

References

[1] S. Iijima, Nature 354 (1991) 56–58.
[2] X. Duan, Y. Huang, R. Agarwal, C.M. Lieber, Nature 421 (2003) 241–245.
[3] Z.W. Pan, Z.R. Dai, Z.L. Wang, Science 291 (2001) 1947–1949.
[4] H. Huang, S. Mao, H. Feick, H. Yan, Y. Wu, H. Kind, E. Webber, R. Russo, P. Yang, Science 292 (2001) 1897–1899.
[5] J.J. Shiang, A.V. Kadavanich, R.K. Grubbs, A.P. Alivisatos, J. Phys. Chem 99 (1995) 17417–17422.
[6] S. Ahmadi, Z.L. Wang, T.C. Green, A. Henglein, M.A. Elsayed, Science 272 (1996) 1924–1925.
[7] C. Liu, J.A. Zapien, Y. Yao, X. Meng, C.S. Lee, S. Fan, Y. Lifshitz, S.T. Lee, Adv. Mater. 15 (2003) 838–841.
[8] Z.S. Wang, C.H. Huang, Y.Y. Huang, Y.J. Hou, P.H. Xie, B.W. Zhang, H.M. Cheng, Chem. Mater. 13 (2001) 678–682.
[9] K. Westermark, H. Rensmo, T.A.C. Lees, J.G. Vos, H.T. Siegbahn, J. Phys. Chem. B 106 (2002) 10108–10113.
[10] H.M. Lin, S.J. Tzeng, P.J. Hsiau, W.L. Tsai, Nanostruct. Mater. 10 (1998) 465–468.
[11] G.M. Hamminga, G. Mul, J.A. Moulijn, Chem. Eng. Sci. 59 (2004) 5479–5485.
[12] J.Q. Hu, Q. Li, N.B. Wong, C.S. Lee, S.T. Lee, Chem. Mater. 14 (2002) 1216–1219.
[13] J.Y. Lao, J.Y. Huang, D.Z. Wang, Z.F. Ren, Nano Lett. 3 (2003) 235–238.
[14] J.Y. Lao, J.G. Wen, Z.F. Ren, Nano Lett. 2 (2002) 1287–1291.
[15] N. Bouropoulos, I. Tsiaoussis, P. Poulopoulos, P. Roditis, S. Baskoutas, Mater. Lett. 62 (2008) 3533–3535.
[16] N.S. Pesika, Z. Hu, K.J. Stebe, P.C. Searson, J. Phys. Chem. B 106 (2002) 6985–6990.
[17] P.V. Radovanovic, N.S. Norberg, K.E. McNally, D.R. Gamelin, J. Am. Chem. Soc. 124 (2002) 15192–15193.
[18] E.W. Seelig, B. Tang, A. Yamilov, H. Cao, R.P.H. Chang, Mater. Chem. Phys. 29 (2003) 257–263.
[19] P. Hoyer, H. Weller, J. Phys. Chem. 99 (1995) 14096–14100.
[20] G.K. Paul, S. Bandyopadhyay, S.K. Sen, S. Sen, Mater. Chem. Phys. 79 (2003) 71–75.
[21] L. Gao, Y.L. Ji, H. Xu, P. Simon, Z. Wu, J. Am. Chem. Soc. 124 (2002) 14864–14865.
[22] B. Cheng, E.T. Samulski, Chem. Commun. (2004) 986–987.
[23] Z. Jia, L. Yue, Y. Zheng, Z. Xu, Mater. Chem. Phys. 107 (2008) 137–141.
[24] D. Qian, J.Z. Jiang, P.L. Hansen, Chem. Commun. (2003) 1078–1079.
[25] K. Simeonidis, S. Mourdikoudis, M. Moulla, I. Tsiaoussis, C.M. Boubeta, M. Angelakeris, C.D. Samara, O. Kalogirou, J. Magn. Magn. Mater. 316 (2007) e1–e4.
[26] Y.C. Zhang, X. Wu, X.Y. Hu, R. Gao, J. Cryst. Growth 280 (2005) 250–254.
[27] X.J.X. Duan, X.T. Huang, E.K. Wang, H.H. Ai, Nanotechnology 17 (2006) 1786–1790.
[28] S.-H. Choi, E.-G. Kim, J. Park, K. An, N. Lee, S.C. Kim, T. Hyeon, J. Phys. Chem. B 109 (2005) 14792–14794.
[29] M. Salavati-Niasari, F. Davar, M. Mazaheri, Mater. Lett. 62 (2008) 1890–1892.
[30] J.F. Liu, Y.Y. Bei, H.P. Wu, D. Shen, J.Z. Gong, X.G. Li, Y.W. Wang, N.P. Jiang, J.Z. Jiang, Mater. Lett. 61 (2007) 2837–2840.
[31] M. Salavati-Niasari, M. Shaterian, M.R. Ganjali, P. Norouzi, J. Mol. Catal. A: Chem. 261 (2007) 147–152.
[32] T. Hyeon, S.S. Lee, J. Park, Y. Chung, H.B. Na, J. Am. Chem. Soc. 123 (2001) 12794–12798.
[33] M. Salavati-Niasari, F. Davar, M. Mazaheri, M. Shaterian, J. Magn. Magn. Mater. 320 (2008) 575–578.
[34] H.T. Yang, Y.K. Su, C.M. Shen, T.Z. Yang, H.J. Gao, Surf. Interface Anal. 36 (2004) 155–160.
[35] J. Park, E. Kang, S.U. Son, H.M. Park, M.K. Lee, J. Kim, K.W. Kim, H.J. Noh, J.H. Park, C.J. Bae, J.G. Park, T. Hyeon, Adv. Mater. 17 (2005) 429–434.
[36] C.V. Yao, H.P. Wu, M.Y. Ge, L. Yang, Y.W. Zeng, Y.W. Wang, J.Z. Jiang, Mater. Lett. 61 (2007) 3416–3420.
[37] Z.R. Tian, J.A. Voigt, J. Liu, B. Mckenzie, M.J. Mcdermott, M.A. Rodriguez, H. Konishi, H.F. Xu, Nat. Mater. 2 (2003) 821–826.